33rd Annual International Conference of the IEEE EMBS
Boston, Massachusetts USA, August 30 - September 3, 2011

An Attempt of Microwave CT System which discriminates the transmission path by means of time domain measurement

Mutsumi TAMURA, Takahiro OGAWA, and Michio MIYAKAWA, *Member, IEEE*

***Abstract*—A microwave-based computed tomography system was developed based on a method that uses time domain measurement to determine the shortest path of propagation components between two antennas. The method calculates shortest path of propagation components by examining mixer output DC components, delivering similar precision as chirp-pulse microwave computed tomography. Because post-mixer signal processing need only concerns DC currents, the effects of overshoot characteristics of baseband filters and the like are removed, simplifying measurement. System circuit composition is also simplified, lowering system costs. This paper provides a theoretical framework for the method, an S-parameter verification of the theory, and an experimental verification using a basic hardware construction. Results showed a restored image from the measurement data, indicating the utility of the method for microwave imaging.**

I. Introduction

Much of the recent research related to microwave imaging of biological bodies has focused on obtaining functional information that cannot be acquired using current tomography systems. Our laboratory's research, too, has until now focused on obtaining functional information that is difficult to obtain using current diagnostic imaging systems such as X-ray computed tomography (CT) when imaging activated brain regions and functioning muscles, or when diagnosing tumors. Previous research has focused on the possibilities related to distribution of temperature variations [1][2], tumor diagnosis [3][4], visualization of activated tissue areas in functioning muscles [5][6], and sugar distribution in fruit [7][8].

To date, our research has been related to the use of chirp-pulse microwave CT (CP-MCT), a method that makes possible tomography through extraction of only straight line propagation components of chirp signals between transmitting-and receiving-antennas in microwave bands [9][10][11]. Because this method allows for the use of chirp signal characteristics in the calculation of the shortest distance paths, careful adjustments of antenna directivity are not required, and thus dipole and other non-directional antennas may be used. Taking advantage of this feature, therefore, makes possible the construction of microwave CT systems employing not only translational- and rotational-scan but also fan-beam scan, providing numerous advantages and extensibility as compared to microwave CT system which works at a constant frequency. On the other hand, sophisticated technology related to microwave chirp signal generators and band-pass filters in the chirp signal wavelength are required. Furthermore, because the sweep capabilities of the chirp signal oscillator affect imaging performance, synchronization between transmitting- and receiving-signals, as well as reduction of noise caused by sweeping, are important issues to be addressed to improve performance. The result is that overall performance of CT relies greatly on the performance of parts and devices related to microwaves. The method for discerning transmission paths using time domain-based measurement presented in this paper entails calculating the shortest transmission paths with the same precision as with a chirp signal, but without using one. Necessary microwave-related hardware includes a transmitting-and receiving-antennas, a signal generator, an RF amplifier, and a mixer. Necessary baseband bandwidth hardware includes a low-pass filter and an A/D conversion circuit. The system is simple to construct, as no special microwave technology equipment is required.

II. Method

Figure 1 shows a system configuration of the transceiver part of the microwave CT system used by the proposed method. A sinusoidal signal is emitted from Antenna A and received by Antenna B. The signal level received by Antenna B will vary according to the electric properties of the object placed between the antennas, and multiple propagation paths will arise as shown in Figure 1. It is therefore necessary to separate out and distinguish only those propagation path components that travelled through the object. The sinusoidal wave oscillator is connected in parallel with Antenna A and mixer terminal 2, and a computer controls the frequency of the oscillator. The first mixer input Terminal 1 receives a signal V_{bi} passing through a bolus. Terminal 1 receives superimposed signals that have passed through multiple propagation paths, and the synthesized signal can be given as shown in Equation 1.

Manuscript received August 27, 2010. This work was supported in part by the Grant-in-Aid for Scientific Research (B) (#22300151) by Japan Society for the Promotion of Science.

M. Tamura is a student at Graduate School of Science and Technology, Niigata University, Niigata, 950-2181 Japan. He is the President with PROCOM.Incorporated, Saitam, 347-0014 Japan. (tamura@procom.jp).

T. Ogawa is a student at Graduate School of Science and Technology, Niigata University, Niigata, 950-2181 Japan. He is the President with MEL Incorporated, Nagoya, 452-0808 Japan. (ogawa@melinc.co.jp).

M. Miyakawa is with the Institute of Science and Technology, Niigata University, Niigata 950-2181 Japan. (miyakawa@eng.niigata-u.ac.jp).

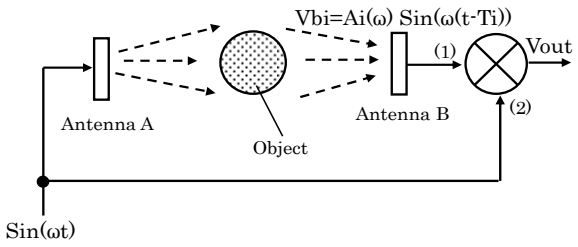

Figure 1. configuration of the microwave CT system.

$$V_b = \sum_{i=1}^{\infty} V_{bi} = \sum_{i=1}^{\infty} A_i(\omega)\sin(\omega(t - T_i)) \quad (1)$$

Here, the subscript *i* indicates the *i*th propagation path. $A_i(\omega)$ is the attenuation coefficient of the *i*th propagation path, a function of the angular frequency ω, and T_i is the propagation delay time of the propagation path. When the mixer is a simple multiplier, the output signal V_{out} will be given by Equation 2, of which Equation 3 is a further expansion.

$$V_{out} = \sin(\omega t)\sum_{i=1}^{\infty} A_i(\omega)\sin(\omega(t - T_i)) \quad (2)$$

$$= \frac{1}{2}\sum_{i=1}^{\infty}[A_i(\omega)\{\cos(\omega T_i) - \cos(2\omega t - \omega T_i)\}] \quad (3)$$

Focusing on the direct current term of Equation 3, this term can be extracted in accordance with Equation 4. Here, because $A_i(\omega)$ is the attenuation coefficient of the *i*th propagation path, $A_i(\omega)$ must be extracted in order to examine the attenuation of the object. Since Equation 4 is a cosine-based periodic function, the behavior of $A_i(\omega)$ can be seen via the relationship $\omega T_i \geq 2\pi$.

$$V_{dcout}(\omega) = \frac{1}{2}\sum_{i=1}^{\infty} A_i(\omega)\cos(\omega T_i) \quad (4)$$

Taking note that Equation 4 is the sum of propagation paths to infinite dimensions, we can use the ω in Equation 4 to perform a Fourier transform, allowing for replacement of V_{dcout} with a function of the propagation path T and enabling discernment of the propagation path. We can therefore use Equation 5 to determine the amplitude of a wave passing through the *i*th propagation path, which when represented in a discrete form results in Equation 6.

$$Vt_{dcout}(T) = \int_{\omega_1}^{\omega_2} V_{dcout}(\omega)\, e^{j\omega T} d\omega \quad (5)$$

$$\hat{V}t_{dcout}(T) = \frac{1}{N}\sum_{k=0}^{N-1} Vt_{dcout}(\omega_k)\, e^{j2\pi k/N}$$

$$= \frac{1}{2N}\sum_{k=0}^{N-1}\{\sum_{i=1}^{\infty} A_i(\omega_k)\cos(\omega_k T_i)\} e^{j2\pi k/N} \quad (6)$$

In Equation 6, $\hat{V}t_{dcout}(T)$ is direct current voltage of the transmitted wave component on each propagation path from zero to infinite. Under the assumed measurement condition, the maximum voltage is observed on the shortest propagation path, i.e. straight path between two antennas. Circular scanning of an object from zero to 360 degrees provides the projection dataset for reconstructing a tomographic image.

III. Experimental Vertification

A. Software-based theoretical verification

To verify the theory presented above, we used a fan-beam imaging system like that shown in Figure 2, measuring the S parameter between the two antennas with a network analyzer and performing the calculation of Equation 6. Using the S parameter to perform numerical calculations allowed exclusion of uncertainty resulting from hardware, which should increase the validity of the theoretical verification. Antenna B in the device had 31 dipole antennas spaced 8 mm apart, which could be toggled using an antenna switch. The distance between Antennas A and B was 176 mm, and a network analyzer was connected between the antennas. A 0.3% saline solution was used as a bolus, and 50 mm and 38 mm diameter cylindrical phantoms were used as objects. The 38 mm phantom was filled with a saline solution of higher concentration than the bolus to increase attenuation. The 50 mm phantom was filled with water to give it attenuation lower than the bolus. Figure 3a shows the results of calculation when using Equation 4 in a variable frequency range from 1 to 2 GHz, and indicates a periodic function like that of Equation 4. The erratic envelop in Fig.3a indicates that multiple propagation paths are present. Figure 3b shows the results of the Fourier transform, corresponding to Equation 6, and depicts the time domain spectrum from 0 to 400 ns. A dominant spectrum was measured at the 76 ns time delay location. Spectra were also confirmed in the vicinities of 125, 275, and 325 ns, indicating that multiple propagation paths were discerned. Figure 4 shows a reconstructed image based on the maximum spectra in the time domain. Figure 4a shows a grayscale image, and Figure 4b shows a three-dimensional representation. Because objects with densities higher and lower than the bolus, were used, the bolus layer is an intermediate level from which positive and negative data can be output.

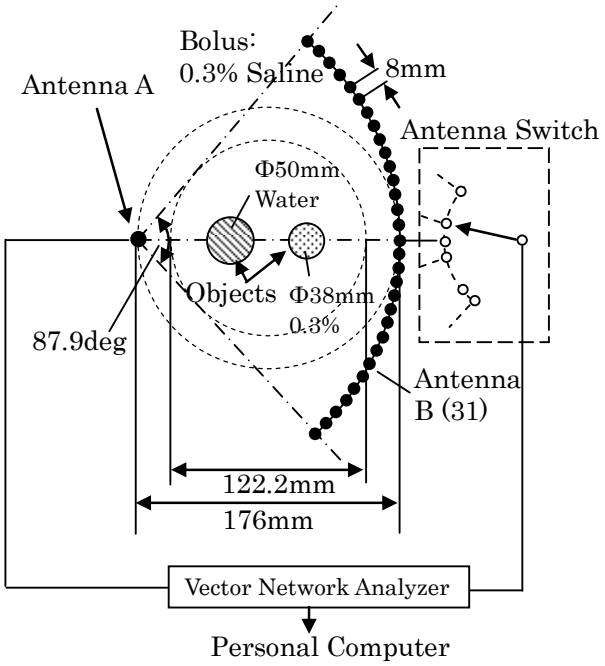

Figure 2. Experimental apparatus with fan-beam device and network analyzer.

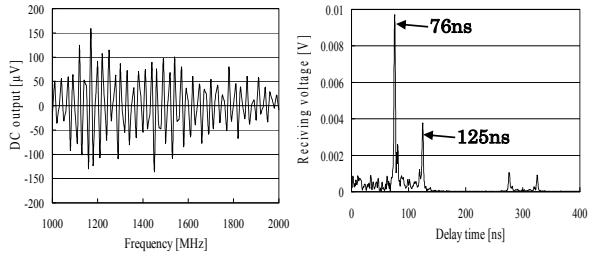

(a) DC output (b) Time domain spectra

Figure 3. DC output and time domain spectra.

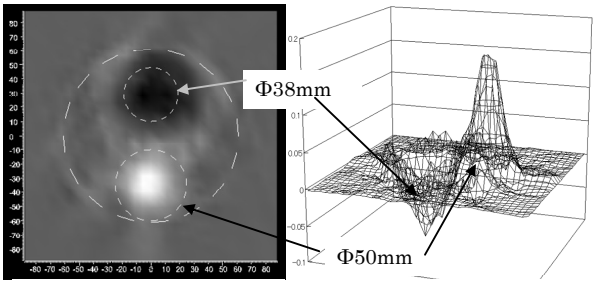

(a) Reconstructed image (b) 3D representation

Figure 4. Reconstructed image and three-dimensional representation.

converter and read by a computer. The output DC signal was read sequentially by using a computer for frequency control, while varying the frequency. The frequency was modulated in 512 points at 2 MHz steps from 978 to 2000 MHz. After reading DC data at each frequency, a Fourier transform was performed according to Equation 6, and the attenuation of the shortest propagation distance was calculated. Figure 6a is a one-dimensional representation of the imaging data, and Figure 6b shows the reconstructed image. The reconstructed image confirms that the object is located in the center. A superimposed circle indicates the size of the object. The image is somewhat small compared to the size of the actual object, but because this is a relative display the size does not carry significant meaning.

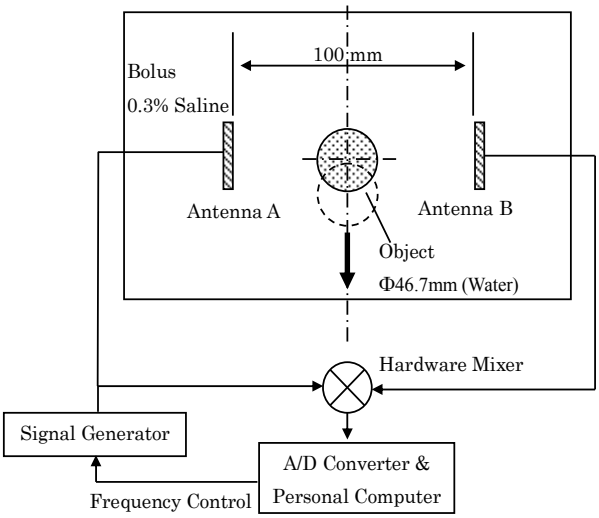

Figure 5. Experimental device with translational beam.

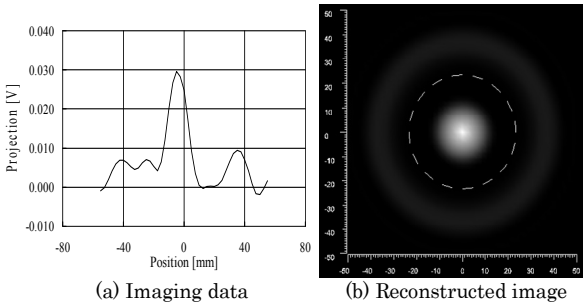

(a) Imaging data (b) Reconstructed image

Figure 6. Imaging data and the reconstructed image.

B. Verification using hardware

In order to verify the proposal system, we used an imaging system with translational scan as shown in Figure 5. Antennas A and B were placed 100 mm apart in a 0.35% saline solution, and a Φ46.7 mm object was placed at the center of the bolus tank between the antennas. An Anritsu MS3633A signal generator was used as a standard signal generator, with an ST Microwave Model 2733B mixer. The DC component of the mixer output was converted to digital data using an A/D

IV. SUMMARY

We developed an algorithm to discern multiple propagation paths as a spectrum along the time axis by focusing on frequency sweeps of sinusoidal wave signals and the periodicity of DC output appearing in homodyne detection output. In order to confirm the validity of the algorithm, we used S parameters measured with a network

analyzer to perform a theoretical investigation. Results confirmed the periodicity of the DC output, and by performing a Fourier transform, we confirmed that propagation paths can be discerned as a spectrum in the time domain. We furthermore confirmed that a reconstructed image can be obtained using the spectrum. The experimental system was developed using basic hardware, confirming that the proposed system can easily be realized from a hardware perspective. Because the proposed method handles only DC components of the mixer output, baseband processing circuitry is simplified, removing the effects of overshoot characteristics from baseband filters and the like, thus making measurements simpler. A further advantage is that the microwave signal does not use a continuously changing signal as in the case of a chirp signal, lessening the importance of the processing speed of signal processing hardware. There is, however, a requirement for flatness in the delay time in the circuitry from the microwave to the baseband.

One remaining problem is that since resolution of the time axis spectrum that discerns the propagation path is in inverse proportion to the sweep frequency width, increasing the resolution requires wide band sweeps. Bolus attenuation, on the other hand, is proportional to the frequency, making wide band sweeps difficult. This means that there is a need for algorithms that can retain propagation path resolution even with narrow band sweeps, making this is a topic for future research.

While the proposed method has unresolved issues related to resolution, we believe that the advantages of being able to discern propagation paths using only DC components are significant, and hope that the method will contribute to the further advancement of microwave CT systems.

ACKNOWLEDGMENT

This work was supported by a Grant-in-Aid for Scientific Research (B) (21340138). We thank Yusuke Sato, a student in the Department of Engineering, Niigata University, for assistance in this research.

REFERENCES

[1] M. Miyakawa, "Visualization of Physiological information or Function of the Biological Body ; New Techniques Used to Visualize Biological Information," IEICE Trans.,77(7), 706-712,1994.

[2] M. Miyakawa, "Microwave imaging—1: Microwave computed tomography," in Non-Invasive Thermometry of Human Body, M. Miyakawa and J. C. Bolomey, Eds., Boca Raton, FL: CRC, pp. 105-126, 1996.

[3] M. Miyakawa, K. Sugawara, M. Bertero and M. Piana, "Computational imaging of the breast- and head-models in CP-MCT," Proc. PIERS 2002 in Cambridge, July 1-5, pp. 593, 2002.

[4] Y. Miyazaki, M. Miyakawa, N. Ishii and M. Bertero, "Analytical study of chirp pulse microwave breast radar (CP-MBR)," 2007 Asia-Pacific Microwave Conference Proc., vol. 2, pp. 597-600, 2007.

[5] M. Miyakawa, T. Yokoo, N. Ishii, and M. Bertero, "Visualization of human arms and legs by CP-MCT," Proc. 38th European Microwave Conference, CD-ROM, pp. 412-415, 2008.

[6] M. Miyakawa, N. Iwata. N. Ishii and M. Bertero, "Low reflection sandwiched dipole array antenna used in high-loss liquids," Proc. 37th European Microwave Conference, pp. 317-320, 2007.

[7] M. Watanabe, M. Miyakawa, Y. Miyazaki, N. Ishii and M. Bertero, "Image restoration of CP-MCT for sugar distribution imaging inside a fruit," Proc. 36th European Microwave Conference, pp. 1248-1251, 2006.

[8] M. Watanabe, M. Miyakawa, "An Attempt of Nondestructive Imaging of Sugar Distribution inside a Fruit Using Microwaves," IEEJ Trans. C, 129(11), 2057-2064, 2009.

[9] M. Miyakawa, D. Watanabe, Y. Saito, "Imaging of the temperature change by the improved chirp rader-type microwave computed tomography," IEEJ Trans. C, 112-C(8), 493-499, Aug. 1992.

[10] M. Miyakawa, "Tomographic measurement of temperature change in phantoms of the human body by chirp radar-type microwave computed tomography," Med. Biol. Engng. Comput., 31(4-S), 31-36, 1993.

[11] M. Miyakawa, "An Attemp of Microwave Imaging of the Human Body by the Charp Rader-Type Microowave CT," IEICE Trans. D, J75-D-II(8), 1447-1454, Aug. 1992.